Geometrical properties of aggregates with tunable fractal dimension



1997 J. Phys. A: Math. Gen. 30 6725

(http://iopscience.iop.org/0305-4470/30/19/013)

J. Phys. A: Math. Gen. **30** (1997) 6725–6735. Printed in the UK PII: S0305-4470(97)81280-2

# Geometrical properties of aggregates with tunable fractal dimension

Romain Thouy and Rémi Jullien

Laboratoire des Verres, Université Montpellier II, Place Eugène Bataillon, 34095 Montpellier, France

Received 24 January 1997

**Abstract.** We have computed geometrical characteristics of large clusters (up to 32 768 particles) obtained by a hierarchical cluster–cluster aggregation computer model in three dimensions, *the off-lattice variable-D model*. Using a 'box-counting' method, we have calculated the fractal dimensions of the surface $D_s$ and the perimeter $D_p$ of their two-dimensional projections as a function of their fractal dimension $D$. By diagonalizing the radius of gyration tensor, we have obtained numerical estimates for the intrinsic anisotropy coefficients (ratios of the eigenvalues) and we have proposed analytical expressions to describe their behaviour as a function of the fractal dimension.

## 1. Introduction

A great number of condensed-matter systems from polymer solutions and colloidal suspensions to smoke and dust, exhibit scale invariance over a large range of lengths. The description of the morphology of such structures by means of fractal geometry [1] has led to a better understanding of the aggregation mechanisms by which they are formed [2, 3] and of their resulting physical and chemical properties [3]. In this paper we are interested by two geometrical problems of great practical importance. The first one is the relation between the characteristics of the two-dimensional projection of a fractal aggregate and its three-dimensional fractal properties. This problem arises, for example, when trying to extract information on a three-dimensional fractal structure from a two-dimensional micrograph, a problem with which many experimentalists were faced. The second concerns the intrinsic anisotropy of a fractal aggregate. While it has been previously shown that the anisotropy is of fundamental importance in fractal aggregated structures [7], such geometrical characteristics, except in some case [8], has seldom been used by experimentalists in connection with fractal properties. In both cases there have been previous theoretical contributions in the literature but they were often confined to particular growth processes. Anisotropy properties of clusters of particles have been studied in some models: random walks [4–6], self-avoiding walks [9], and lattice animals and percolation [7, 10–12].

In this paper we address these two problems numerically with fractal aggregates which have been built on a computer using a newly developed off-lattice hierarchical model with a tunable fractal dimension [14]. This quite general model can be considered as an extension of the existing cluster–cluster aggregation models with different cluster trajectories [2, 3] since the cluster penetration is here chosen to obtain the desired fractal dimension. In section 2 we present a numerical study of the fractal characteristics of the

0305-4470/97/196725+11$19.50  

two-dimensional projections. In particular we calculate the fractal dimension of both the bulk and the perimeter of the projection as a function of the fractal dimension of the three-dimensional cluster. In section 3 we present a numerical study of some intrinsic anisotropy characteristics of the clusters. After diagonalizing the radius of gyration tensor, we calculate the anisotropy coefficients which are the ratios between the successive eigenvalues. Based on an approximate expansion in $(D-1)$, we propose an analytical expressions for the dependence of these coefficients with the fractal dimension. In section 4 we discuss these results and conclude.

## 2. Numerical study of the aggregate projections

### *2.1. Principles*

We have previously published results about the calculations of 'effective' fractal dimensions for the surface $D_s$ and the perimeter $D_p$ of the two-dimensional projections of fractal aggregates obtained by the on-lattice version of the variable-$D$ model [15]. But, since we have developed an off-lattice version of this model which is able to build more realistic fractal aggregates [14], we have judged it useful to reproduce such a calculation using this new version. Moreover, instead of calculating 'effective' fractal dimensions (which were obtained by comparing aggregates of successive sizes) here we have calculated the fractal dimensions using a more standard 'box-counting' method, close to the numerical methods used by experimentalists to analyse their micrographs.

For each aggregate, we have stored its projections on planes perpendicular to the $x$, $y$, and $z$ directions of the three-dimensional space. As the aggregates are made of hard spheres of diameter 1, some of which are on contact, their projections are made of circles, some of which are overlapping. On the projection plane we have defined a square grid with mesh $\ell$, where $\ell$ is the edge length of an individual square or 'pixel'. Then we have defined the 'occupied' pixels as being located either on the perimeter or inside the surface of the aggregate. Such occupied pixels are lying completely inside the circular projection of a particle (for small $\ell$) or are such that at least one of their edges is cut by at least one circle. Then, among all the occupied pixels, we have counted the numbers $N_s$ and $N_p$ of pixels respectively located inside the surface and on the perimeter of the projection, a pixel inside the surface being such that all its nearest neighbours are occupied.

The procedure has been performed with different $\ell$ values, we have recovered the scaling relations

$$\begin{aligned} N_p &\sim \ell^{-D_p} \\ N_s &\sim \ell^{-D_s}. \end{aligned} \tag{1}$$

We have found that such scaling holds between $\ell_{min} \simeq 1.5$ and $\ell_{max} \simeq 0.07N^{1/D}$ where perfect straight lines are found in a log–log plot.

### *2.2. Results and discussion*

We have performed several runs on samples up to $N = 32\,768$ particles, with a tunable fractal dimension ranging from 1.1 to 2.5. For each run, we have taken 40 different values of $\ell$ which allowed us to fit the log–log curves using standard linear regression methods. We have averaged all the calculations over 16 samples for clusters of size $N = 8192$ (open symbols), and over four samples for clusters of size $N = 32\,768$ (full symbols), and for each one, over the three-projection axis.

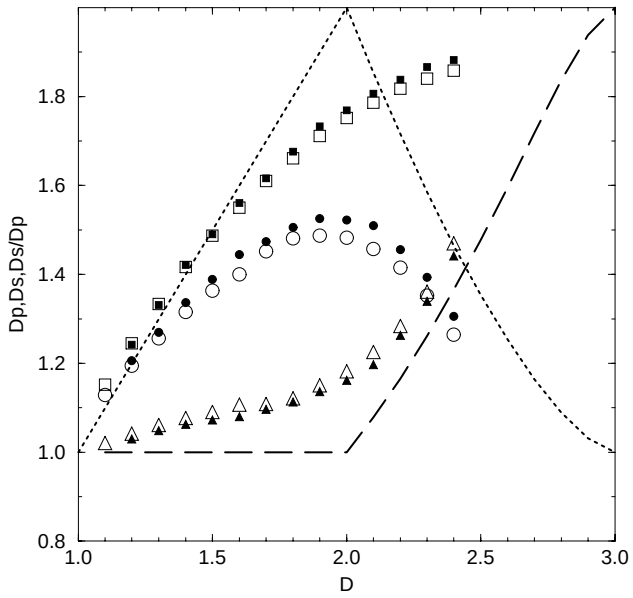


**Figure 1.** Numerical results for the fractal dimensions $D_s$ (square), $D_p$ (circle) and $D_s/D_p$ (triangle) as a function of $D$, for $N = 8192$ (open symbols) and $N = 32\,768$ (full symbols). Dotted and broken curves indicated the conjectures for $D_p$ and $D_s/D_p$ (equations (2) and (3)).

All the estimated slopes $D_p$, $D_s$ and $D_s/D_p$ are reported in figure 1. On the same figure we have indicated by broken and dotted curves the conjectures made in our previous work [15], for $2 < D < 3$:

$$D_p = 1 + (3 - D)^{\frac{3}{2}} \tag{2}$$

$$\frac{D_s}{D_p} = \frac{2}{1 + (3 - D)^{\frac{3}{2}}}. \tag{3}$$

We recall that, in [15], this conjecture was obtained by extrapolating to infinite size an effective fractal dimension which was defined in order to attenuate finite-size corrections [18]. Here, when using the box-counting method, it turns out that the finite-size effects are considerably larger since one observes on figure 1 that, even for such a large value as $N = 32\,768$, the curves for both $D_s$ and $D_p$ stay far from their asymptotic and/or estimated values. Note that the finite size effects are larger in the vicinity of $D = 2$ and larger for $D_p$ than for $D_s$. Finite-size effects are even present for small $D$ (close to one) where we could have expected to recover $D_s = D_p = D$ with a good accuracy.

## 3. Intrinsic anisotropy of clusters

### *3.1. Method*

Here we follow the numerical procedure first introduced by Hentschel [16]. We write the radius of gyration tensor $R^2_{i,j}$ [7] for a given cluster with $N$ particles, as:

$$R^2_{i,j} = \frac{1}{N}\sum_{n=1}^{N}(x_i^n - x_i^0)(x_j^n - x_j^0) \tag{4}$$

where $x_i^n$ denoted the $i$th coordinate ($1 \leqslant i \leqslant 3$) of the $n$th particle and $x_i^0$ denoted the $i$th coordinate of the mass centre. The eigenvalues obtained by diagonalizing this tensor define the principal radii of gyration $R_i^2$ ($i$ now labels the eigenvalues). We put them in the following conventional order:

$$R_1^2 \geqslant R_2^2 \geqslant R_3^2. \tag{5}$$

Taking into account the invariance of the trace of the tensor $R_{i,j}^2$, we have

$$\sum_{i=1}^{3} R_i^2 = \sum_{i=1}^{3} R_{i,i}^2 = R^2 \tag{6}$$

where $R$ is the usual radius of gyration which verifies the scaling relation:

$$R^2 \sim N^{2/D}. \tag{7}$$

Assuming constant anisotropy ratios between the eigenvalues, the scaling relation is also verified by each $R_i$. Using the hierarchical procedure of the variable-$D$ model [13], we have built, in three dimensions, aggregates of 32 768 particles, with fractal dimensions ranging from 1.1 to 2.5. The eigenvalues $R_1^2$, $R_2^2$ and $R_3^2$ have been averaged over the whole collection of clusters of $2^k$ particles at several step $k$ of the iterative procedure (typically, we choose $k = 8$–11, to get a good average). To characterize the anisotropy, we have calculated the ratios:

$$A_1 = \frac{\langle R_1^2 \rangle}{\langle R_3^2 \rangle} \tag{8}$$

$$A_2 = \frac{\langle R_2^2 \rangle}{\langle R_3^2 \rangle} \tag{9}$$

where $\langle \ldots \rangle$ denotes the average over all the collection of clusters. In addition, we have also calculated the anisotropy ratio $A_1'$, defined as in equation (8), for random two-dimensional projections of the three-dimensional fractal clusters. Botet *et al* [17] have previously studied the anisotropy ratio, for three different cluster–cluster aggregation processes (in two, three and four dimensions). The present work extends these results for clusters with tunable fractal dimensions, and propose some extrapolation for the behaviour of $A_1$, $A_2$ and $A_1'$ as a function of the fractal dimension.

### *3.2. Results*

A first qualitative estimate of the effect of the fractal dimension on the anisotropy can clearly be seen by looking at the two-dimensional projections of the three-dimensional aggregates depicted in our previous papers [13, 14]. To be more quantitative here, we have reported, in the log–log plot of figure 2, the values obtained for $A_1$ (circles) and $A_2$ (squares) as a function of $(D - 1)$, for two cluster sizes $N = 1024$ and 2048 (open and full symbols respectively), averaged over 128 and 64 clusters (respectively). For comparison, we have indicated the results found by Botet *et al* [17] for three-dimensional aggregates in the case of linear trajectories: $A_1 = 10.0 \pm 0.3$ and $A_2 = 2.5 \pm 0.3$ (full triangles), for a fractal dimension $D = 1.98$. They are in a good agreement with our results. Indeed we find a strong dependence of the anisotropy with the fractal dimension. When $D \to 1$, $A_1$ increases dramatically while $A_2$ turns out to saturate to a finite value, of about 7. Note that the dependence of the numerical results with the size is very small, therefore the values reported for the anisotropy ratios can be estimated to be very close to their asymptotic large-$N$ limit.

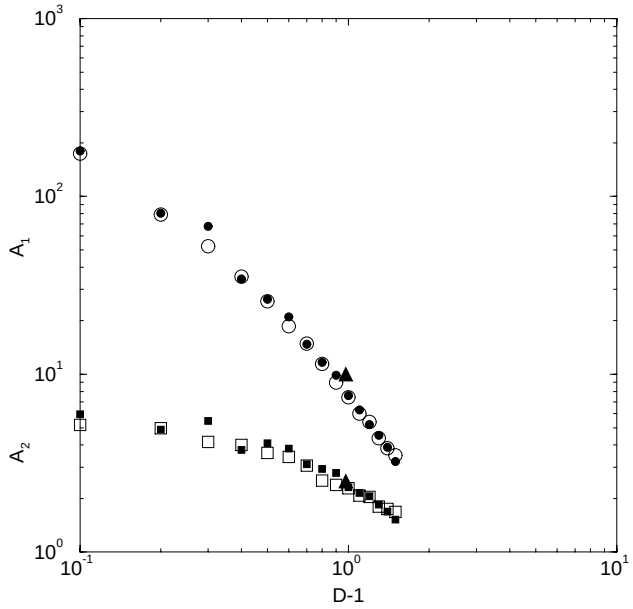


**Figure 2.** Log–log plot of $A_1$ (circle) and $A_2$ (square) as a function of $(D-1)$, the data have been averaged over 128 and 64 clusters for $N = 1024$ (open symbols) and 2048 (full symbols), respectively. Full triangles are the values of $A_1$ and $A_2$ are taken from [17].

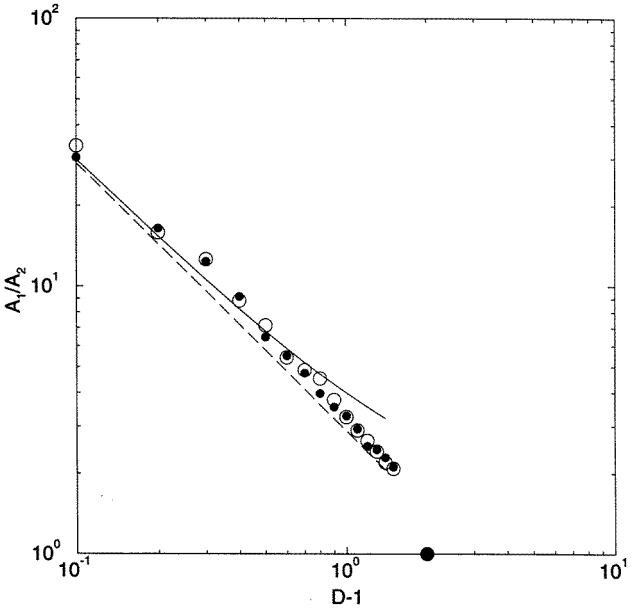


**Figure 3.** Log–log plot of the ratio $A_1/A_2$ as a function of $(D-1)$ for $N = 1024$ (open circles) and 2048 (full circles). The data have been averaged over 128 and 64 clusters, respectively. The full curve and the broken straight line correspond to equations (19) and (20), respectively.

In figure 3, we have reported the ratio $A_1/A_2$ as a function of $(D-1)$ in a log–log plot, for $N = 1024$ and 2048 (open and full circles respectively). This plot reveals a quasilinear dependence which can be expressed as:

$$\frac{A_1}{A_2} \simeq \frac{3}{D-1}. \tag{10}$$

Note that this approximate relation cannot be valid up to $D = 3$ since one should get $A_1/A_2 = 1$ (point indicated by a full circle in figure 3) in this spherically isotropic limit. However, we recall that our model could not go beyond an upper fractal dimension, estimated to be $D_M = 2.55$ for $d = 3$, and this is the reason why we have not reported any data above this limit.

Finally, we have used the algorithms of section 2 and 3, to calculate the radii tensor of the three projections of aggregates, and, by diagonalizing this tensor, we have obtained their principal radii of gyration which allowed us to calculate $A_1'$, the anisotropy ratio for a two-dimensional projection of a three-dimensional cluster. The determination of $A_1'$ was the same as the method employed for $A_1$ and $A_2$ calculations, but for each projection, we have taken into account all the centres of squares, with edge length $\ell = 2$, used to encompass the aggregate projection. For each aggregate projection, we performed first the dressing determination, and then, the calculation of $A_1'$. An average over the three projections has been done at the end of the procedure. Typically, we have averaged the results over 32 samples for $N = 1024$ particles, and over 16 samples for $N = 2048$ particles (taking into account the three projections, we have done in fact an average over 96 and 48 samples respectively). We have plotted our results on figure 4, versus $(D-1)$, in log–log scale. We added previous results for other cluster–cluster models, namely $A_1' \simeq 4.4$ and 4.0 respectively for Brownian (full square) and linear trajectories (full diamond and triangle). These results are extracted from [17] and the note added therein. There is a good agreement with our results. Another remark is that the behaviour of $A_1'$ looks similar to that of $A_1/A_2$, suggesting also a divergence proportional to $1/(D-1)$ as $D \to 1$ but with a larger coefficient:

$$A_1' \simeq \frac{5}{D-1}. \tag{11}$$

In the next section we will try to understand the $D$ behaviour of all these anisotropy coefficients by performing some approximate calculations valid in the strong anisotropic limit $D \to 1$.

### *3.3. Discussion*

We recall that the variable-$D$ model is an iterative cluster–cluster aggregation procedure. This procedure builds fractal clusters of $2N$ particles by randomly joining two clusters of $N$ particles. It also satisfies the constraint that the distance $\Gamma$ between the centres of mass $G_1$ and $G_2$ stays proportional to the mean quadratic radius of gyration $R$ (i.e. $R^2$ is the mean squared radius of the two clusters):

$$\Gamma = kR \tag{12}$$

where $k$ is a function of the input fractal dimension:

$$k = 2\sqrt{4^{1/D} - 1}. \tag{13}$$

Knowing that the radius of gyration $R'$ of the new cluster of $2N$ particles is given by [18]:

$$R'^2 = R^2 + \Gamma^2/4 \tag{14}$$

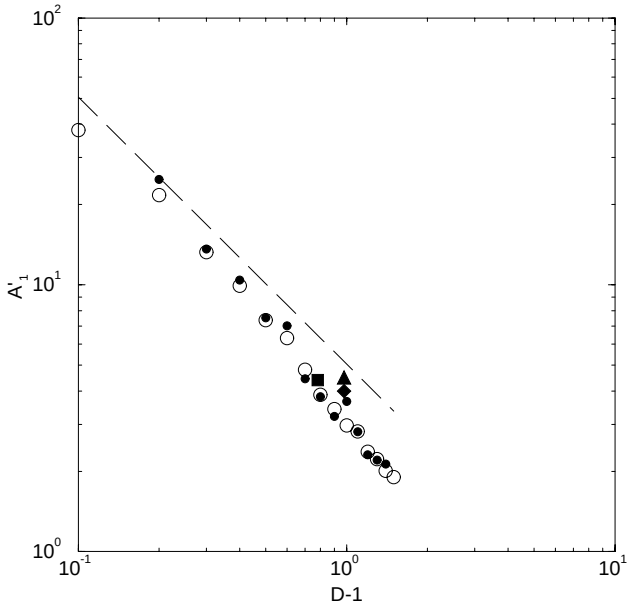


**Figure 4.** Log–log plot of $A'_1$ as a function of $(D-1)$ for $N = 1024$ (open circles) and 2048 (full circles). The data have been averaged over 128 and 64 clusters, respectively. We have added results taken from [17] for the cluster–cluster aggregation model with Brownian (full square) trajectories and with linear trajectories (full diamond and triangle).

it can be checked that the sticking rule is consistent with the scaling relation:

$$R' = 2^{1/D} R. \tag{15}$$

Note that here we have dropped some finite-size corrections which were present in the original model (in order to have $R = 0$ for $N = 1$) [15] but which become irrelevant for large $N$ values.

In the strong anisotropy limit $D \to 1$, one has $k \to \sqrt{12}$ and $R'_1 \to 2R_1$ while $R_2 \ll R_1$ and $R_3 \ll R_1$. In that limit the sticking point $I$ is located near the tips of the two clusters almost on their principal axis (corresponding to their larger radius of gyration) and the principal axis of the two clusters make infinitesimal angles $\theta_1$ and $\theta_2$ (see figure 5, left) with the principal axis (1') of the new cluster which is almost in the direction $G_1G_2$. Assuming (consistently with the scaling hypothesis) a strict proportionality between maximum radii and gyration radii and considering a sticking point $I$ located right on the tips, projecting on (1') and taking the average of the principal radius of gyration squared over the $\theta_1$ and $\theta_2$ orientations, one obtains:

$$R'^2_1 \simeq 4R_1^2 \langle \cos^2 \theta \rangle. \tag{16}$$

Comparing with the scaling relation which should hold for the three eigenvalues, one obtains:

$$\langle \cos^2 \theta \rangle \simeq \frac{4^{1/D}}{4} \tag{17}$$

which is indeed an approximate estimation of the mean disorientation only valid in the limit $D \to 1$, $\theta \to 0$.

We will now assume that the second eigenaxis (2') of the new cluster (corresponding to the second eigenvalue $R'_2$), perpendicular to (1'), is almost in the plane $G_1G_2I$, due to

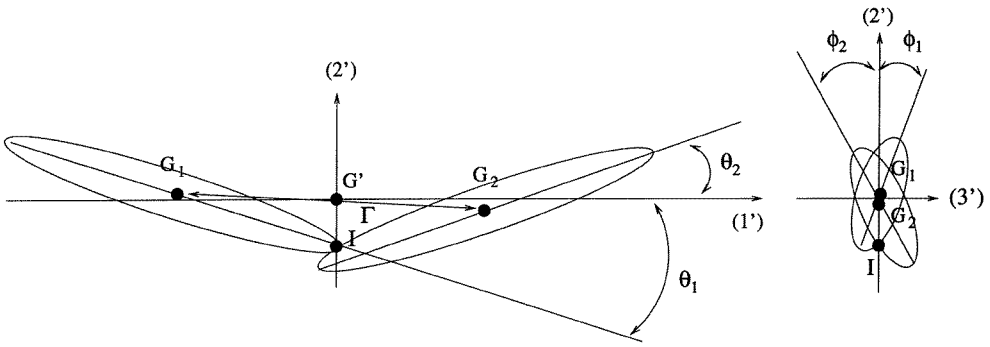


**Figure 5.** Sketch of the sticking of two aggregates of $N$ particles to give a larger aggregate of $2N$ particles in the limit $D \to 1$. The aggregates are represented by ellipsoids. The principal axis of the resulting aggregate are (1') (2') (3'). $G_1$, $G_2$ and $G'$ denote the centres of mass and $I$ the contact point. Left and right correspond to projections in the plane (1') (2') and (2') (3'), respectively.

the small disorientation. Then, neglecting the intrinsic lateral extensions of the two clusters and projecting on (2') in a similar way to above, one obtains:

$$R'^2_2 \simeq R_1^2 \langle \sin^2 \theta \rangle. \tag{18}$$

Using the scaling relation for $R_2$ and the result for $\langle \cos^2 \theta \rangle$, one obtains:

$$\frac{A_1}{A_2} = \frac{1}{4^{-1/D} - \frac{1}{4}}. \tag{19}$$

This relation is indicated by the full curve in figure 3. In view of the crude reasoning, the agreement with the numerical data turns out to be very good. As expected the agreement is better for values of $D$ close to 1. When expanding this relation in terms of $(D-1)$, one obtains:

$$\frac{A_1}{A_2} = \frac{2/\ln 2}{D-1} \simeq \frac{2.88}{D-1} \tag{20}$$

to be compared with equation (10). This expansion is reported as the broken straight line in figure 3. The better agreement with the numerical data should be considered as fortuitous as the numerical values should deviate below the previous curve to get $A_1/A_2 = 1$ for $D = 3$.

To estimate $R'_3$, one should now consider a projection onto a plane perpendicular to (1') (see figure 5, right). We recall that, in this plane, the direction of (2') is almost determined by the projection of the plane $G_1G_2I$. We will assume that the principal axis of the two cluster projections are the second axis of the three-dimensional clusters and make angles $\phi_1$ and $\phi_2$ with (2'). Note that, although they should be both smaller than $\pi/2$ (due to the small disorientation mentioned above), these two angles cannot be considered as very small. We will even assume that, in the limit $D \to 1$ where $\theta_1$ and $\theta_2$ vanish, $\phi_1$ and $\phi_2$ become uniformly random. Projecting on the direction (3') (which is perpendicular to (1') and (2')) and averaging in the same way as above, one obtains:

$$R'^2_3 = R_2^2 \langle \sin^2 \phi \rangle + R_3^2 \langle \cos^2 \phi \rangle. \tag{21}$$

Then using the scaling relation for $R_3$ and assuming $\langle \sin^2 \phi \rangle = \langle \cos^2 \phi \rangle = \frac{1}{2}$, one obtains:

$$A_2 = 2.4^{1/D} - 1. \tag{22}$$

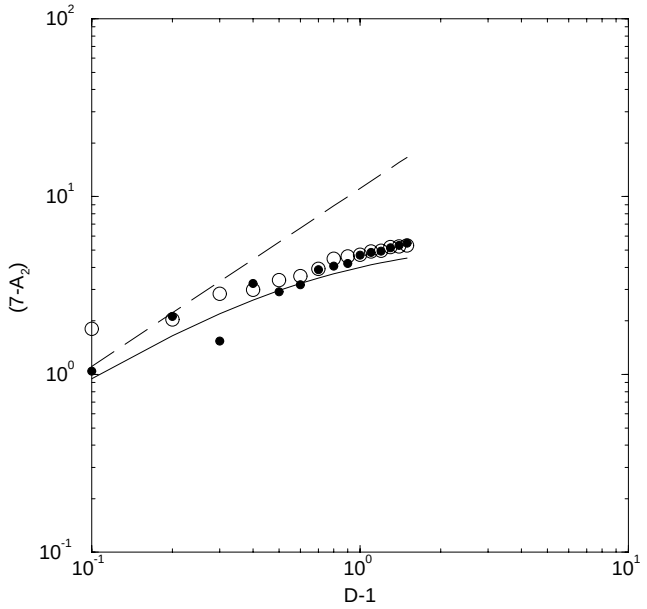


**Figure 6.** Log–log plot of $(7 - A_2)$ as a function of $(D - 1)$ for $N = 1024$ (open circles) and 2048 particles (full circles). The data have been averaged over 128 and 64 clusters respectively. The full curve and the broken straight line correspond to equations (22) and (23), respectively.

It is remarkable to obtain $A_2 \to 7$ when $D \to 1$ as observed in the numerical results. In figure 6, we compare the numerical data for $A_2$ with this theoretical formula as well as with the $(D - 1)$ expansion

$$A_2 = 7 - 8(D - 1)\ln 4. \tag{23}$$

Here again the agreement is quite good.

At last, in the same spirit, we can give an approximate relationship between the anisotropy coefficient of the two-dimensional random projection $A_1'$ and those of the three-dimensional clusters. Assuming that, in the strong anisotropic limit, the principal axis of the projection is the projection of the principal axis of the three-dimensional cluster which makes a random angle $\psi$ with the projection plane, the largest eigenvalue of the projection is $R_1^2\langle\cos^2\psi\rangle = R_1^2/2$, i.e. half of one of the three-dimensional clusters. With the same reasoning, since the projection angles of the other axis are also random, the second eigenvalue is half of the average of $R_2^2$ and $R_3^2$. This gives:

$$A_1' = \frac{2A_1}{1 + A_2}. \tag{24}$$

Using the results for $A_1/A_2$ and $A_2$, $A_1'$ should diverge as:

$$A_1' = \frac{7/(2\ln 2)}{D - 1} \simeq \frac{5.04}{D - 1}. \tag{25}$$

This expansion, which is very close to formula (11), corresponds to the broken straight line shown in figure 4.

## 4. Conclusion

In this paper, we have calculated some geometrical characteristics of fractal aggregates built with the off-lattice variable-$D$ model, namely the fractal dimensions of the surface and perimeter of two-dimensional projections and the intrinsic anisotropy ratios of both the aggregates themselves and their projections. We have studied how these characteristics vary as a function of the fractal dimension of the clusters and have been able to give approximate analytical expressions in some cases. Concerning the fractal characteristics of the two-dimensional projections, we have found that they were subject of strong finite-size corrections and therefore the experimental study of these quantities alone in specific cases might not be so useful to extract precise information on the fractal dimension. We have seen that, even for fractal dimensions smaller than two, the fractal dimension cannot be estimated from the fractal characteristics of two-dimensional projections, calculated with the box-counting method, in contrast with what is commonly admitted. On the other hand, the anisotropy parameters seem to be quite insensitive to size and they strongly depend on the fractal dimension. In particular we have found that the anisotropy ratio of a random two-dimensional projection decreases when increasing the fractal dimension, roughly proportionally to the inverse of $(D-1)$. Since the experimental determination of such a parameter can be very easy in many cases, it can provide a simple indirect way to estimate the variation of the fractal dimension of cluster aggregates. However, when trying to more quantitatively apply our results to any experimental situation, it should be remembered that they are not universal, in the sense that they have been calculated for a particular cluster–cluster model in which cluster polydispersity has been neglected. This lack of universality was previously mentioned in our earlier paper [15] when we were introducing the conjectured formulae (2) and (3) for the dependence of the fractal dimensions of surface and perimeter of a projection on the bulk fractal dimension. However, it has been pointed out to us that, surprisingly, these formulae work nicely for percolation clusters [19] which have obviously nothing to do with the variable-$D$ model. Anyway, before applying our results to any experimental situation, it would be worth having some evidence that the growth process of the observed aggregates is of cluster–cluster type and that cluster polydispersity can be neglected.

## Acknowledgment

Calculations were done at CNUSC (Centre National Universitaire Sud de Calculs, Montpellier, France).

## References

[1] Mandelbrot B B 1982 *The Fractal Geometry of Nature* (San Francisco, CA: Freeman)
[2] Jullien R and Botet R 1987 *Aggregation and Fractal Aggregates* (Singapore: World Scientific)
[3] Meakin P 1988 *Adv. Colloid Int. Sci.* **28** 249
[4] Kuhn W 1934 *Kolloid Z.* **68** 2
[5] Solc K 1971 *J. Chem. Phys.* **55** 335
[6] Bishop M and Michels J P J 1985 *J. Chem. Phys.* **82** 1059
[7] Family F, Vicsek T and Meakin P 1985 *Phys. Rev. Lett.* **55** 641
[8] Allain C and Jouhier B 1983 *J. Physique* **44** L421
[9] Rudnick J and Gaspari G 1986 *J. Phys. A: Math. Gen.* **19** L191
[10] Freche P, Stauffer S and Stanley H 1985 *J. Phys. A: Math. Gen.* **18** L1163
[11] Garik P 1985 *Phys. Rev.* A **32** 1275

[12] Lam P M 1986 *J. Phys. A: Math. Gen.* **19** L155
[13] Thouy R and Jullien R 1994 *J. Phys. A: Math. Gen.* **27** 2953
[14] Thouy R and Jullien R 1996 *J. Physique* I **6** 1365–76
[15] Jullien R, Thouy R and Ehrburger-Dolle F 1994 *Phys. Rev.* E **50** 5
[16] Hentschel H G E 1984 *Kinetics of Aggregation and Gelation* ed F Family and D P Landau (Amsterdam: Elsevier) p 117
[17] Botet R and Jullien R 1986 *J. Phys. A: Math. Gen.* **19** L907–12
[18] Ball R and Jullien R 1984 *J. Phys. Lett.* **45** L1031
[19] Stauffer D 1995 Private communication